Electronic structure of many-electron square-well quantum dots with and without an attractive impurity: Spin-density-functional theory

Bhalchandra Pujari,[1,2,*] Kavita Joshi,[1] D. G. Kanhere,[1,2] and S. A. Blundell[3]
[1]*Department of Physics, University of Pune, Ganeshkhind, Pune 411 007, India*
[2]*Centre for Modelling and Simulations, University of Pune, Ganeshkhind, Pune 411 007, India*
[3]*Département de Recherche Fondamentale sur la Matière Condensée, CEA-Grenoble/DSM, 17 rue des Martyrs, F-38054 Grenoble Cedex 9, France*
(Received 21 April 2007; published 24 August 2007)

The electronic structure of many-electron square-well quantum dots with and without an attractive impurity has been investigated within the spin-density-functional theory. We consider various sizes of quantum dots with the number of electrons varying from 2 to 20. We observe the emergence of localized Wigner-molecule-like behavior along with the wall-like feature in the charge density. However, unlike the parabolic quantum dots, we do not observe the analog of concentric rings. We also observe the typical broken symmetry configurations noted in earlier reports for quantum dots. The impurity induces the localized magnetic moment which, in many cases, generates the spin-polarized configurations with the antiferromagnetic coupling. An examination of the magnetic states indicates that the presence of impurity may change the ground state of quantum dot from magnetic to nonmagnetic and vice versa. We also observe that the localized charge at the center sharpens the walls.

DOI: 10.1103/PhysRevB.76.085340 PACS number(s): 73.21.La, 71.55.−i, 75.30.Fv, 71.10.−w

I. INTRODUCTION

Understanding the basic physics of low dimensional systems and, in particular, the nanomaterials has gained an immense importance because of their technological implications. Quantum dots are zero dimensional electron systems experimentally realizable due to advances in the fabrication technology. Because of their similarities with the atomic structures, they are considered as *the artificial atoms*.[1–3] Such quantum dots, formed by confining two dimensional gas, are highly tunable in terms of the number of electrons and the size. Therefore, they represent important paradigms for investigating various properties of interacting many-body systems. The applications vary from single-electron transistor, spectral detectors, lasers to even quantum computing. Equally interesting are possible novel quantum effects due to electron-electron interactions and confinement. Since their realization in early 1980s,[4] quantum dots have been a subject of extensive theoretical[3,5] and a variety of experimental investigations.[1,2]

In recent years, electronic structure of quantum dots has been investigated by a variety of techniques. A majority of the work reported is with the parabolic confining potentials.[3] There have been several well established studies on quantum dots using density functional theory (DFT) and spin density functional theory (SDFT).[3,6–8] Considerable insight has been gained because of extensive DFT investigation in spite of the limitation of such a one-electron approach. One of the success of DFT is to reproduce the addition spectra for the quantum dots observed experimentally.[9,10] The magnetic component of the ground state depicted by the DFT, which results in shell structure of quantum dots, is also in agreement with the Hund's rule.[10] Even the highly correlated features such as Wigner localizations have been successfully picked up by the DFT.[6,7] For an exhaustive review on electronic structure of quantum dots, we refer to the article by Reimann and Manninen.[3] We also refer to the work of Farrelly and co-workers[11,12] on the localization of one and two point lattice limits with field induced boundaries.

The reports on DFT have also brought out some features which are subject of extensive debate, e.g., the broken symmetry solutions. In the low density regime, mean field theories may lead to the solutions in which spin density does not follow the rotational symmetry of the confining potential. Yannouleas and Landman[13] have analyzed and classified the symmetry breaking in quantum dots at zero or low magnetic field, while Harju *et al.*[14] have presented a general scheme that incorporates several configurations into DFT to restore the symmetry.

In addition, such theories are also known to fail to reproduce the results in the strongly correlated regime. In spite of such limitations, considerable insight has been gained because of extensive DFT investigations, and DFT based methods remain one of the easily accessible methods in treating large number of electrons. It may be noted that for a proper treatment of electron-electron correlations, sophisticated techniques like configuration interaction[5] and quantum Monte Carlo (QMC)[15] are warranted. A recent work by Ghosal *et al.*[16,17] using QMC has pointed out an interesting aspect, namely correlation induced inhomogeneity in quantum dots.

Although quantum dots are usually modeled by considering the external confinement to be parabolic in shape, the current technology enables us to engineer other types of confinements also[18] e.g., ellipsoidal, square, polygonal, etc. Such investigations with different confining geometries help to bring out a class of features which are generic to the confinement. Akbar and Lee[6] have studied up to 12-electron square quantum dot describing addition energy spectra, charge configuration, and Wigner-molecule-like states. Studies have also been carried out on rectangular and some other polygonal confinements.[19]

It turns out that the quantum dots are prone to have impurities during the process of fabrication. Quite clearly, the presence of even a single impurity or disorder is bound to affect the electronic properties of the dot. Therefore, a thorough understanding of the effect of impurity on the electronic structure is highly desirable.[20–22] Reusch and Egger[23] have used the path integral Monte Carlo to study the impurity effect on the quantum dots. Their focus has been the incipient Wigner molecule regime. Räsänen *et al.*[22] have studied the effect of an impurity placed in the vicinity of quantum dot on the single-electron transport spectrum. They use parabolic confinement with parameters adjusted to yield experimental one-electron spectrum. The impurity is considered to be a negatively charged Coulombic one. Their SDFT calculations are restricted to six electrons. They have observed that the impurity evens out the state alteration as a function of magnetic filed. Şahin and Tomak[20] have studied the electronic structure of spherical quantum dot with an impurity. They have seen that the capacitive energy with the impurity increases with respect to the case without impurity. Studies on off-center hydrogenic impurity have been carried out by Movilla and Planelles.[21]

In the present work, we have calculated electronic structure of square-well quantum dots with weak, attractive impurity placed at the center of the dot. We carry out an extensive DFT analysis of charge and spin densities by varying electrons from 2 to 20 and over a wide range of dot sizes. Typical r_s range considered here is from 0.5 to 10.

The paper is organized in the following manner. We describe the model of the quantum dot and impurity in the following section (Sec. II). We also draw the details of computational work in the same section. We summarize our results on pure quantum dot in Sec. III A where we present the density profiles, the magnetic state of the system, etc. Section III B describes the results obtained by inserting the impurity and contrasting these results with the pure system. Finally, in the last section (Sec. IV), we summarize our results.

II. MODEL AND COMPUTATIONAL DETAILS

A. Pure system

The quantum dot is defined as a system of interacting electrons in an external confinement taken as a square-well potential in the present case. The quantum dot under investigation is strictly two dimensional (confined in the z axis), so the external potential takes the form

$$V_{ext}(x,y) = \begin{cases} 0, & 0 \geqslant x \geqslant L,\ 0 \geqslant y \geqslant L \\ V_0 & \text{otherwise}, \end{cases} \tag{1}$$

where L is the length of the quantum dot and the barrier height $V_0 = 1200$ meV. The material of the dot is assumed to be GaAs. We also assume effective mass approximation with an effective mass $m^* = 0.067 m_e$, where m_e is the mass of an electron, and dielectric constant $\epsilon = 12.9$. The units of length and energy are scaled to effective atomic units: effective Bohr radius $a_B^* = 9.8$ nm and effective hartree $\mathrm{Ha}^* = 2\mathrm{Ry}^* = 12$ meV. In the SDFT formalism, the Schrödinger equation in Kohn-Sham[24,25] scheme reads as

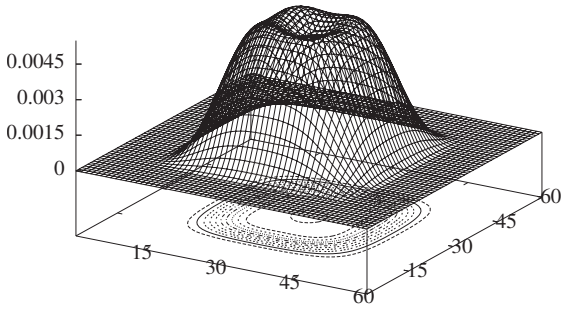

FIG. 1. The charge density of the four-electron system constructed out of noninteracting particle eigenfunctions using Hund's rule ($S_z = 1$). The qualitative nature of the charge density will remain unchanged for all values of r_s.

$$\left(-\frac{\hbar^2}{2m^*}\nabla^2 + V_{eff}^{\sigma}(\mathbf{r}) \right) \psi_i^{\sigma}(\mathbf{r}) = \epsilon_i \psi_i^{\sigma}(\mathbf{r}), \tag{2}$$

where V_{eff}^{σ} is the effective potential with spin σ. We define the density parameter r_s as

$$r_s = L\sqrt{\frac{1}{\pi N}}. \tag{3}$$

It is clear from this equation that for higher density, r_s is lower and vice versa.

We use real-space grid technique for the solution of Eq. (2). For exchange-correlation energy, we use the local density approximation.[26] Our technique initiates the self-consistency with one of the several hundred educated guesses of charge density in search of energy minima, which assures the detection of actual ground state of the system.

We first take a look at the single-particle (noninteracting) picture in this potential. For such a system, wave functions are given by

$$\psi_{n_x,n_y} = \frac{2}{L}\cos\left(\frac{n_x \pi x}{L}\right)\cos\left(\frac{n_y \pi y}{L}\right), \tag{4}$$

and energy eigenvalues by

$$E_{n_x,n_y} = \frac{1}{2}(n_x^2 + n_y^2). \tag{5}$$

Following the notation used by Akbar and Lee[6] we see the degeneracy in the eigenspectra as (s), (p_x, p_y), (d_{xy}), $(d_{x^2-y^2}, 2s)$, and so on. Now, using this single-particle eigenstates and Hund's rule ($S_z = 1$), a typical four-electron density is generated and is shown in Fig. 1. The qualitative nature of this density remains unchanged for all sizes of quantum dot (i.e., with respect to the variation in r_s).

B. Impurity model

We model our impurity in a simple Gaussian form

$$V_{imp}(x,y) = -Ae^{-\beta(x^2+y^2)}. \tag{6}$$

We add this V_{imp} to the external potential given in Eq. (1). Parameters A and β can be used to tune the impurity for

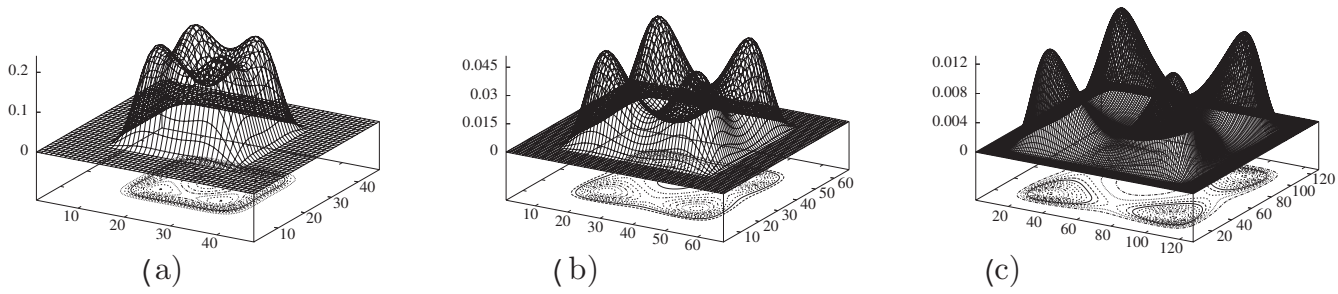

FIG. 2. The total charge densities of the four-electron quantum dot for (a) $r_s \sim 1.5$, (b) $r_s \sim 4$, and (c) $r_s \sim 8$.

desired results. We set $A=12$ meV and $\beta=0.5$. Radius of the impurity is ~35 nm. Throughout the calculations described in this paper, we maintain this set of parameters unchanged. The parameters are so adjusted that the impurity has a bound state for noninteracting case, while it has no bound state in the many-body picture. We have placed the impurity at the center of the dot.

Such kind of impurity can be present while fabricating the quantum dot by the subsistence of positive charges or it can well be engineered to seek the exciting properties. Experimentally, it is already seen that the external positive charges can create a "bubble" in charge density of two dimensional electron gas.[27]

III. RESULTS

A. Pure system

As discussed in the Introduction, there have been some studies on the square quantum dots.[6,7,19] In order to place the impurity results in proper perspective, we briefly present the main features observed in the pure systems for the number of electrons varying from 2 to 20.

1. Charge density profile

We have carried out an extensive SDFT study for various sizes of the quantum dot. We vary r_s by varying one of the quantities, namely, the number of electrons or the length of the dot, keeping the other fixed. The first set of calculations is carried out for four different fixed sizes with length of the side $L \sim 45$, 100, 210, and 315 nm, and for each of these cases, self-consistent solution has been obtained for $N=2-20$. The second set of calculations has been carried out for the systems up to 20 electrons for two different values of r_s, namely, 1.5 and 4.

It is instructive to bring out the difference between the noninteracting charge density shown in Fig. 1 and the SDFT charge density shown in Fig. 2. The figure shows the total charge density for the four-electron case for three different values of r_s, i.e., $r_s \sim 1.5$ [Fig. 2(a)], 4 [Fig. 2(b)], and 8 [Fig. 2(c)]. It is evident from Fig. 2(a) that, in higher density region, the SDFT picture is in fair agreement with the noninteracting one. However, as r_s increases (low density region), the SDFT charge density begins to differ considerably from the noninteracting one. Indeed, as seen from Fig. 2(c), the SDFT charge density captures the highly localized behavior characteristics of *Wigner-molecule-like behavior*.[3,5,12,14,28–32] In confined systems at low densities, the confinement strength weakens and the Coulomb interaction dominates, leading to such a localization.

It is to be noted that the square well has four characteristic points, namely, its corners. Whenever the number of electrons (either up, down, or total) is less than or equal to 4, they arrange themselves in the four corners of the well in the form of localized peaks in the low density region. As the number of electrons increases, there is a general tendency for the formation of *walls* along the sides of the dot. In Fig. 3, we plot the total charge densities with $N=2$, 6, 11, and 20 electrons for the case of high density region (left panel) and low density region (right panel). As can be seen from the figure, once these four corners of the well are occupied by four electrons, the excess electrons tend to spread themselves not only toward the corners but also along the sides of the well forming wall-like structures.

It is interesting to note that the charge density along the walls is *inhomogeneous*. This can be brought out by examining the evolution of the charge density along the wall as a function of number of electrons by keeping the area fixed. In Fig. 4, we show the charge density along the line joining the two adjacent peaks (along the walls) for five different values of the number of electrons. The figure shows the oscillating nature of the total charge density and the emergence of more than one peak for the large values of electron count, e.g., $N=20$. It is to be expected that for a large number of electrons (area remaining constant), the number of oscillations will increase yielding almost uniform wall. It is evident from Figs. 3(c) and 3(d) that the oscillations become more significant in low density region. In this density region, the wall structures correspond to *semilocalized* electrons, i.e., they are considerably localized in the direction perpendicular to sides while along the sides they are delocalized. It is reasonable to expect that in the extremely low density region, the oscillations noted above will emerge as clearly localized peaks.[35]

2. Spin-polarized densities

Because of their single-determinantal approximation to the full many-body ground state wave function, the mean field theories are known to yield the broken symmetry solutions. Such symmetry breaking solutions in quantum dots have been analyzed in great detail[3,7,13,33] for zero and low magnetic fields. The system breaks the internal symmetry and gains the exchange-correlation energy resulting a typical

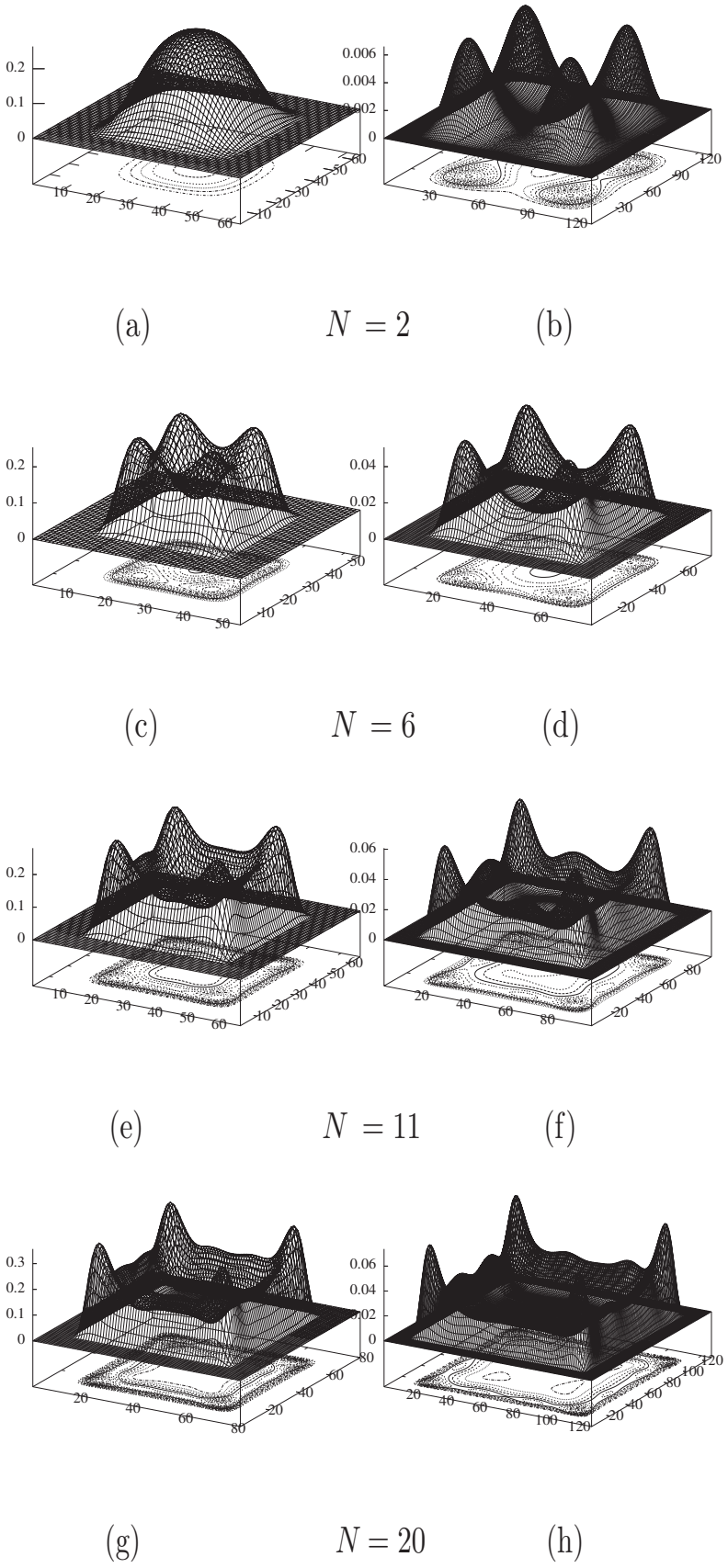

FIG. 3. Total charge densities in high density region (left panel) and in low density region (right panel) for $N=2$, 6, 11, and 20. High density region corresponds to $r_s \sim 1.5$, and low density region corresponds to $r_s \sim 4$ except for $N=2$, where $r_s \sim 12$.

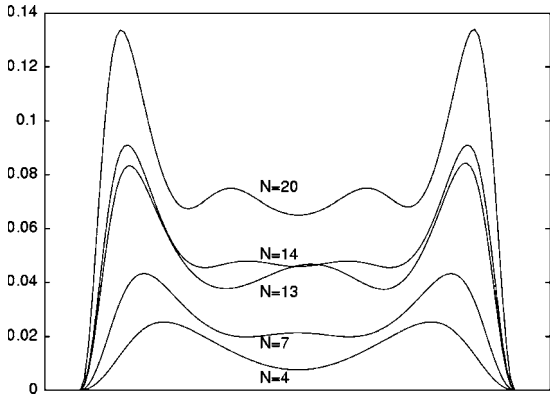

FIG. 4. Oscillations of the charge density along a side of the well. The size of the well is fixed to be ~250 nm, so r_s varies from ~6 (for $N=4$) to ~2.7 (for $N=20$).

spin-density-wave-like solution.[7] Although a broken symmetry solution is the issue of substantial debate,[3] such a solution gives considerable insight into the nature of the charge density.

Our spin-polarized solutions can generally be categorized into three classes. First is a trivial case where the solutions for up and down electrons are the same. In this case up, down and total charge densities confirm the rotational symmetry of the confining potential. Second is the case where up and down charge densities are different but all the charge densities follow the symmetry of the confining potential, and the third class is where only the total charge density has the desired rotational symmetry.

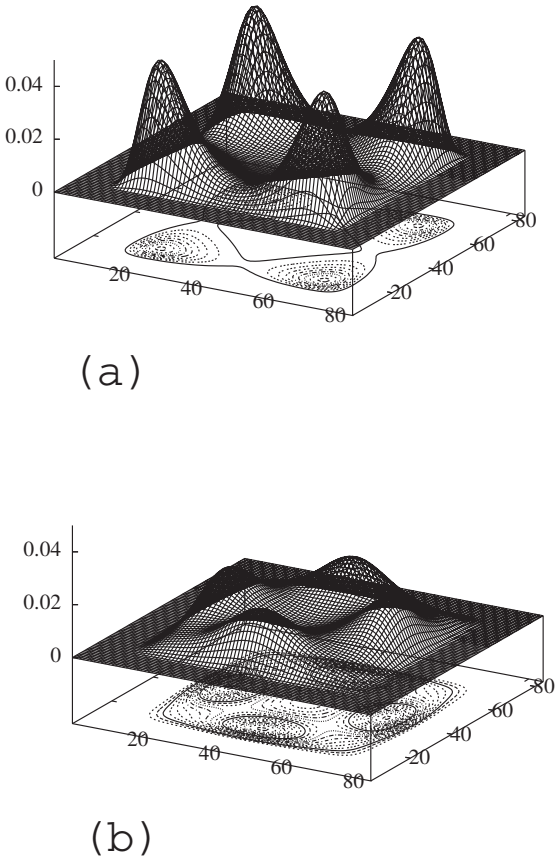

FIG. 5. Spin-density-wave-like behavior observed for $N=7$, $S_z=1/2$, and $r_s\sim4$. The charge densities for (a) four up electrons and (b) three down electrons are rotated by an angle $\pi/4$ with respect to each other, giving rise to SDW-like configuration.

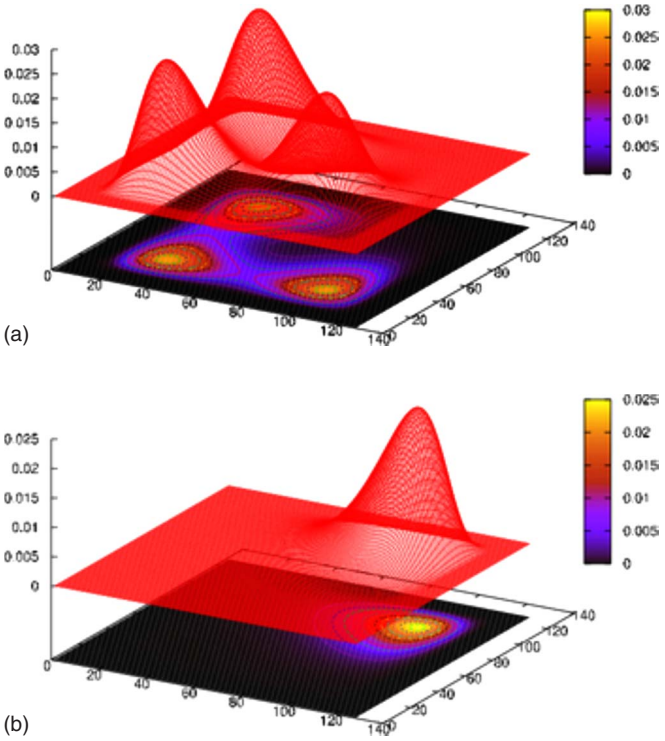

FIG. 6. (Color online) The charge densities for three up (a) and one down (b) electrons of the four-electron quantum dot for $S_z=1$ at $r_s\sim4$. This is the broken symmetry solution, where individual spins do not follow the symmetry of the potential.

The charge density belonging to the second class is illustrated in Fig. 5. In this figure, we show the charge density of seven-electron quantum dot at $r_s\sim4$, where four up electrons localize themselves at the four corners [Fig. 5(a)] and the remaining three electrons are arranged along the walls [Fig. 5(b)], in such a way that their charge density is shifted by $\pi/4$ with respect to the up electron charge density. It may be noted that these down electrons are considerably less localized. Thus, in this case, the spins are antiferromagnetically ordered.

Figures 6(a) and 6(b) show the charge density belonging to the third class for $N=4$ at $r_s\sim4$. The ground state belongs to $S_z=1$. Clearly, this is the broken symmetry solution where three up electrons are localized in the three corners and one down electron is localized in the remaining corner. It may be noted that the total charge density has the desired symmetry. Such broken symmetry solution is predominantly observed in the lower density region.

3. Magnetic states

Our SDFT scan of the solutions for various values of r_s and N shows that the quantum dots display a variety of magnetic states and transitions from one state to another. This

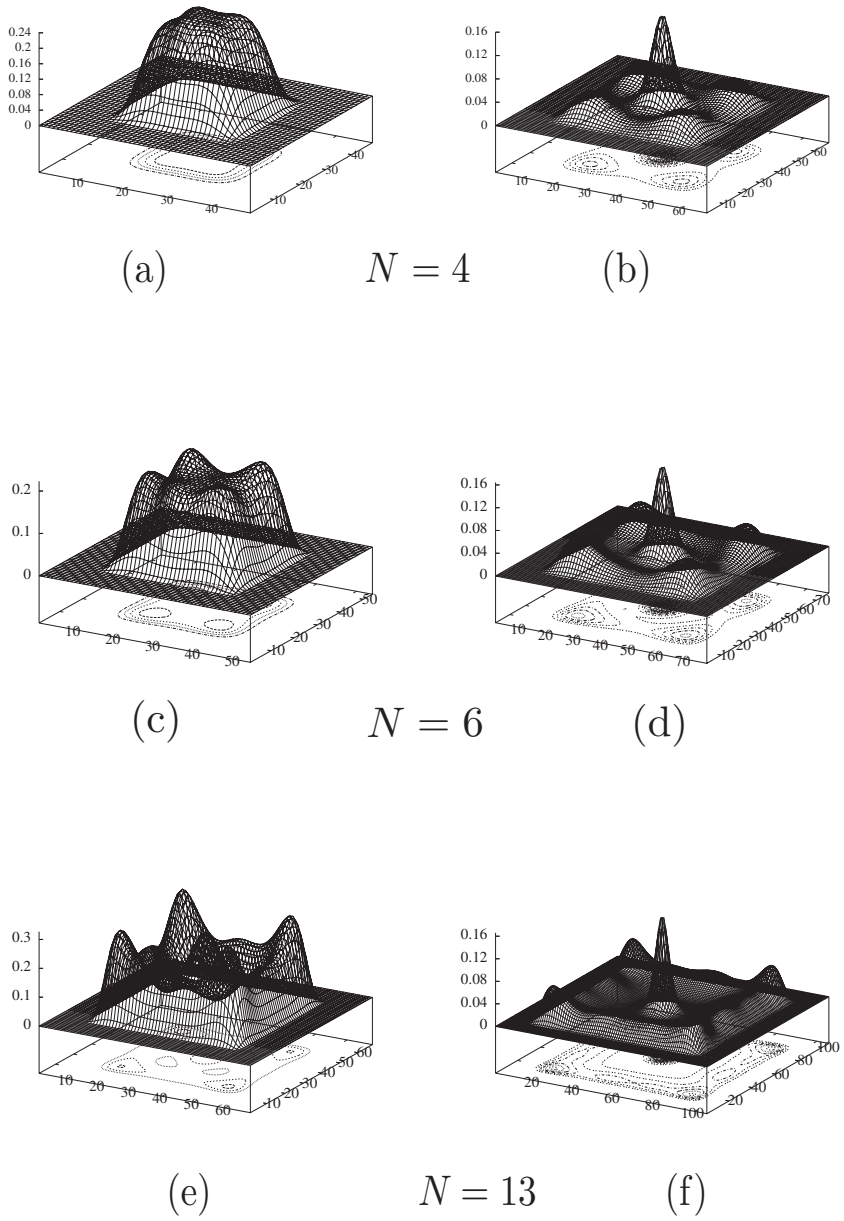

FIG. 7. Left and right panels show the total charge density in the high density ($r_s \sim 1.5$) and low density ($r_s \sim 4$) regimes, respectively, for N=4, 6, and 13 electron quantum dot.

observation is consistent with the earlier report by Akbar and Lee.[6] In general, in high density region (dot size ~65 nm), shell filling of electrons is in accordance with the noninteracting spectra (discussed in Sec. II A). Thus, N=4, 10, 14, and 18 the ground state has S_z=1, in agreement with the Hund's rule. However, with the expansion of the dot, the SDFT eigenspectra start departing from simple noninteracting spectra significantly and magnetic transitions occur. We summarize the values of S_z for the ground state in Table I. In this table, we have noted the cases where the magnetic state has changed as a function of area. There is no obvious trend that can be drawn from this table.

TABLE I. Magnetic states (S_z) for two different sizes of quantum dot.

No. of electrons	S_z for $L \sim 65$ nm	S_z for $L \sim 250$ nm
3	$\frac{1}{2}$	$\frac{3}{2}$
4	1	0
5	$\frac{1}{2}$	$\frac{3}{2}$
10	1	0
12	0	1
13	$\frac{1}{2}$	$\frac{3}{2}$
19	$\frac{1}{2}$	$\frac{3}{2}$
20	0	2

B. Quantum dot with an impurity

Now, we present the results with the addition of impurity by contrasting them with those obtained in the pure system.

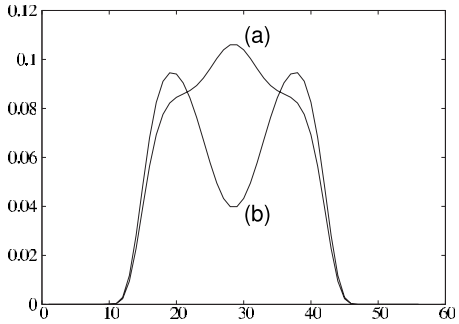

FIG. 8. The down ($N_{\downarrow}=3$) charge density of the seven-electron dot plotted along the diagonal of the well ($r_s \sim 1.5$). (a) Charge density in the presence of the impurity and (b) without impurity.

Our parameters are identical to those described in Sec. II B irrespective of the size of the well.

1. Charge density profile

It is expected that due to the presence of an attractive impurity, the charge will be accumulated at the center. As we shall see, this will have a significant effect on the charge density especially in the low density regime. In Fig. 7, we show the total charge densities of $N=4$, 6, and 13 at $r_s \sim 1.5$ (left panel) and $r_s \sim 4$ (right panel) in the presence of the impurity. For four-electron quantum dot in the high density regime, the impurity is covering a substantial area ($\sim 90\%$) within the dot. As a consequence, the eigenfunctions and the charge density are totally dominated by the attractive potential of the impurity resulting in nearly uniform charge density covering the impurity region. As we increase the number of electrons (keeping r_s fixed), the size of the dot also increases. Slowly, we see the formation of four peaks ($N=6$), and eventually for higher number of electron ($N>6$), we see the formation of a small peak at the center. The presence of the impurity thus induces the peak in the charge density at the center of the dot. This feature is absent in the pure system. The evolution of the charge density is brought out in Fig. 8, where we have shown the down electron charge density along the diagonal with and without impurity for the seven-electron system.

For the low density regions (left panel of Fig. 7), the central peak can be seen for all the electrons. For high value of r_s, the strength of the confinement reduces and the area covered by the impurity becomes modest in comparison with the area of the dot. In this regime, electrons start loosing their kinetic energy and tend to get away from each other to minimize the Coulomb repulsion. Eventually, only one electron (either up or down) gets "trapped" inside the impurity and others spread in the remaining area of the well [Fig. 7(b)]. The charge densities for higher number of electron are shown in Fig. 7 for $r_s \sim 1.5$ and 4. The development of wall-like feature observed in the case of pure quantum dot (Sec. III A 1) is also seen in the present case, however, with a difference. Note that, in the case with impurity, we have five special points, namely, four corners and one impurity site at the center, so that the building of wall-like feature starts for $N>5$. Because of the presence of a localized charge at the center, the electrons along the borders of the well feel extra Coulombic repulsion. This makes walls and the corners sharper, i.e., more localized as compared to the pure system.

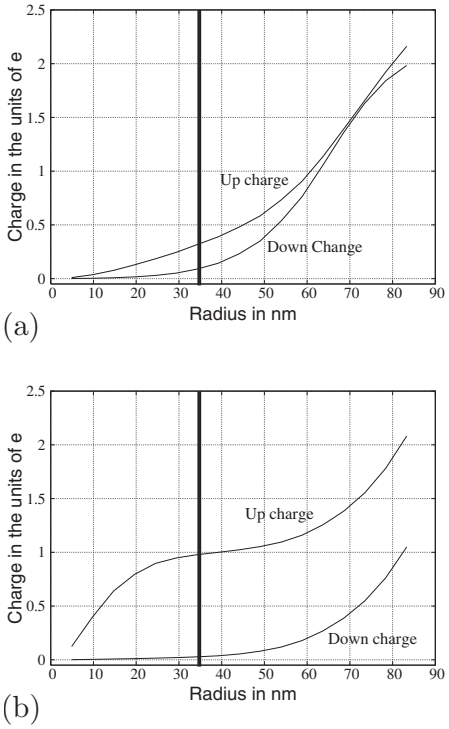

FIG. 9. Charge enclosed within the radius (up to ~85 nm), in case of $N=11$ ($S_z=1/2$, $r_s \sim 4$), for (a) system without impurity and (b) system with impurity. Observe that only one up electron is trapped within the impurity radius (~35 nm, shown by vertical bar) and other electrons are getting pushed away.

To illustrate the nature of the localization of an electron in the impurity region, we compute the charge enclosed within a circle of radius r, centered at the impurity. In Figs. 9(a) and 9(b), we show the up and down charges enclosed within the radius r for pure system and system with impurity, respectively. The plot is for $N=11$ ($S_z=1/2$) and the vertical bar represents the extent of the impurity. As can be seen, there is hardly any charge near the center in absence of the impurity; however, impurity induces the total charge of 1, and as a consequence, other charges are repelled from the center. Interestingly, the effect of the impurity is to place the localized magnetic moment $\left(S_z=\frac{1}{2}\right)$ at the center and has interesting implications in the magnetic order, which is discussed in the next section.

2. Spin-polarized densities

It is of some interest to examine the possible magnetic order. In the presence of impurity, we have three general classes of spin polarization, like those in the pure system. However, it is interesting to note some differences in the spin density. Most of the systems in the high density regime fall under the trivial class of spin-unpolarized case, so we focus our discussion on the low density regime. We begin the discussion by presenting a simple two-electron case. It is known[7] that two-electron dot at low densities displays the

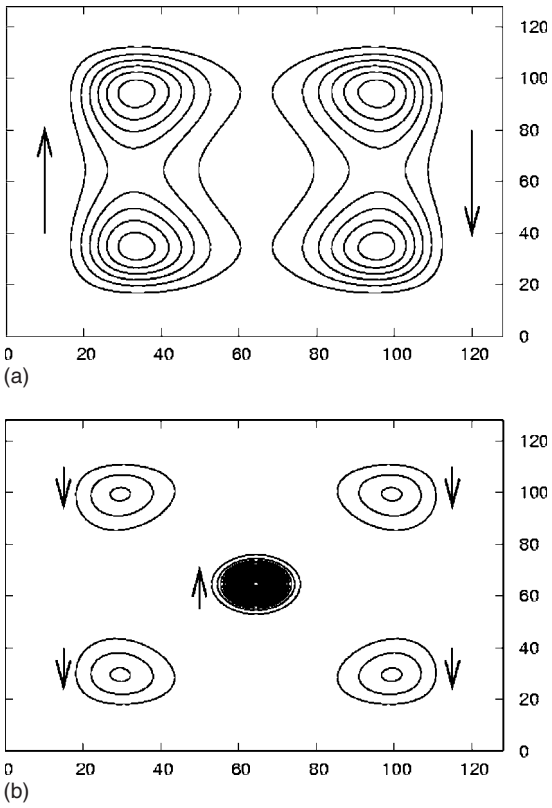

FIG. 10. Charge density contours of the two-electron quantum dot for $S_z=0$ at $r_s\sim 12$ for (a) the pure system and (b) the system with impurity.

spatial separation of up and down spins (broken symmetry solution of type 3 of Sec. III A 2). Figure 10 shows the charge density contours for up and down spins: (a) without impurity and (b) with impurity for a typical low density region (dot size ~300 nm). As the impurity potential is turned on, one of the electron, say up, is firmly localized at the center while the other one (down) is localized at the four corners, generating antiferromagnetic-like coupling between the center and the corners. Note that in the presence of impurity, both the spin densities follow the symmetry of the potential. This can be contrasted with the behavior of the corresponding case of the pure system shown in Fig. 10(a).

The spin ordering for $N=3$ and 4 is similar to that shown in Fig. 10(b). The excess electrons get distributed in the corners. The dots with $N=5$, 6, and 7 belong to the broken symmetry solution, where individual spin densities do not follow the symmetry of the potential (figure not shown).

The dots with $N=8$, 9, and 10 belong to the second class of solution where up and down spin densities separately follow the symmetry of the potential but are not identical. A typical case for $N=10$ is illustrated in Fig. 11. In this figure, we show the spin density $(\rho_\uparrow-\rho_\downarrow)$ for ten-electron system ($S_z=0$, $r_s\sim 4$). It can be seen that one of the down electrons is trapped inside the impurity and the remaining four down electrons are localized at the corners and the five up electrons form the wall. The peaks in the up spin density lie in between the corresponding peaks of down spin density. The eigenspectrum for this system is shown in Fig. 12, where it is clearly seen that only one eigenstate for down electron lies

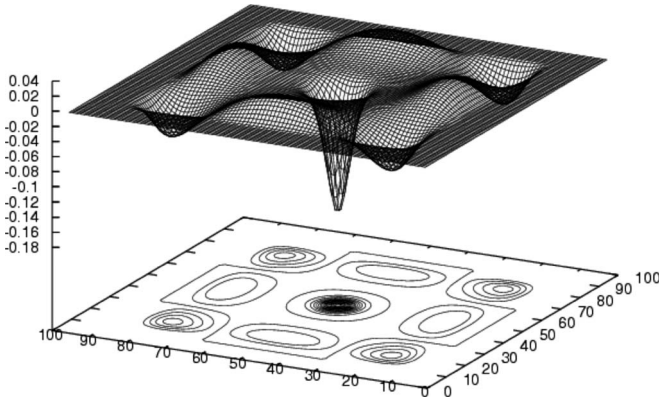

FIG. 11. Spin density $(\rho_\uparrow-\rho_\downarrow)$ of the ten-electron quantum dot with impurity for $S_z=0$ at $r_s\sim 4$.

far below the rest of the spectrum (singly occupied). The impurity also causes the bunching (near degeneracies) of states as seen in the figure.

3. Magnetic states

The presence of the localized charge (in the present case, a localized magnetic moment) may alter the magnetic state of the corresponding homogeneous quantum dot. Table II summarizes the results with and without impurity for two distinct values of r_s, namely, 1.5 and 4. In this table, we have shown only those cases where impurity has changed the magnetic state (S_z) of the system with respect to the pure

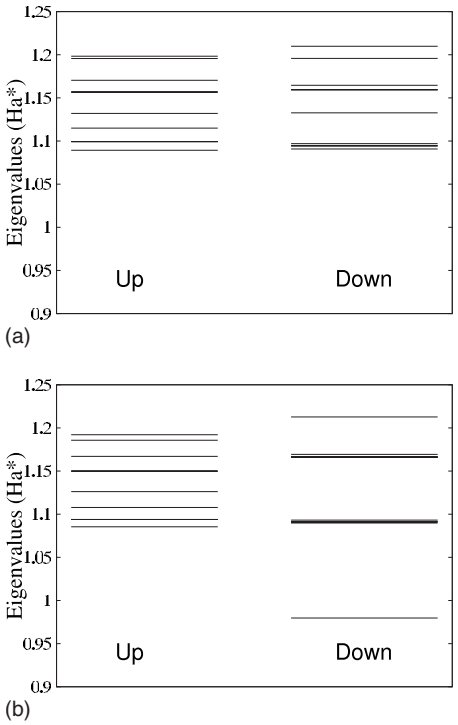

FIG. 12. Eigenvalue spectrum without (a) and with (b) impurity for $N=10$ and $r_s\sim 4$ $(S_z=0)$. Difference in up and down spectra in pure case (a) is because of the presence of SDW-like spin arrangement. Observe the appearance of single separate eigenstate in the down spectrum for impure dot (b).

TABLE II. Transition of magnetic states of the quantum dot with impurity.

	$r_s \sim 1.5$		$r_s \sim 4$	
N	S_z for pure	S_z for impure	S_z for pure	S_z for impure
3	$\frac{1}{2}$	$\frac{1}{2}$	$\frac{3}{2}$	$\frac{1}{2}$
4	1	1	0	1
5	$\frac{1}{2}$	$\frac{1}{2}$	$\frac{3}{2}$	$\frac{1}{2}$
6	0	0	0	1
7	$\frac{1}{2}$	$\frac{1}{2}$	$\frac{1}{2}$	$\frac{3}{2}$
8	0	0	0	1
13	$\frac{3}{2}$	$\frac{1}{2}$	$\frac{3}{2}$	$\frac{3}{2}$
14	1	1	0	1
18	1	0	0	1
19	$\frac{3}{2}$	$\frac{1}{2}$	$\frac{1}{2}$	$\frac{1}{2}$
20	0	0	2	1

system. It can be seen that the impurity has the significant effect on the low density region ($r_s \sim 4$). Surprisingly, the impurity also alters the magnetic states of a few cases in the high density region (e.g., $N=13$, 18, and 19), reducing the values of S_z. Thus, the impurity may be used to change the magnetic state of the quantum dot from high to low as well as from low to high. For example, for $N=3,5,20$, the impurity changes the spin state from high to low. Experimentally, such transitions have been achieved by means of suitable external magnetic field.[34]

4. Addition spectra

The *addition energy* of the nth electron is defined as

$$\Delta_n = E_{n+1} - 2E_n + E_{n-1}, \tag{7}$$

where E_n is the total energy of the nth electron. Addition energy is the amount of energy required to add an electron to the dot. Thus, the higher the value of Δ_n, the more stable is the n-electron dot. We present the calculated addition energy spectra for the dot size of $\sim$105 nm without and with impurity in Fig. 13. This size spans the r_s from 1.3 (for $N=20$) to 4.3 (for $N=2$). As can be seen from the figure, the addition spectra of the quantum dots with small number of electrons are significantly affected by the impurity.

IV. SUMMARY

The electronic structure of square quantum dot with and without an attractive impurity has been calculated within the framework of SDFT. The results have been obtained for charge density, spin density, total energy, and magnetic moment of the ground states for number of electrons ranging from 2 to 20 and for several values of r_s.

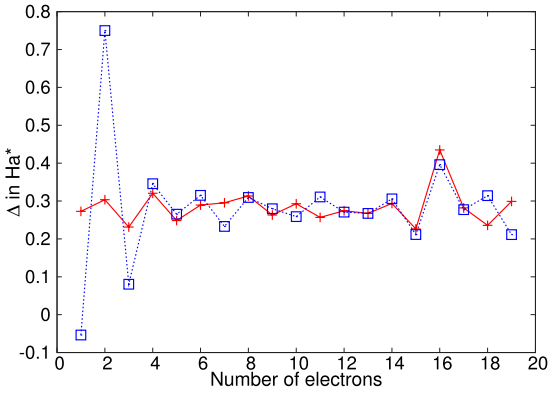

FIG. 13. (Color online) Addition spectra with (dotted line) and without (solid line) impurity for well size $\sim$105 nm.

We observe localized charge density characteristic of the low density regime. Typically, in the present case, the charge density shows four peaks which are associated with the walls for higher number of electrons. Unlike in the case of parabolic confinement where concentric rings are observed, we do not observe such a concentric set of walls. We also observed spin density wave SDW-like configurations for a class of parameters.

The impurity is seen to induce the significant changes in charge density especially in central region. For two to four electrons, we observe an antiferromagnetic-like configurations with firm unit magnetic moment at the center and four peaks at the corners for opposite spins. It is also observed that the magnetic state of the dot changes due to the presence of the impurity.

Finally, it may be mentioned that the picture evolved in the present work is based on a single-particle-like approach. It is known that in the low density regime, the electron-electron correlation effects are significant; therefore, wherever possible, it is desirable to verify the results by explicitly correlated methods such as configuration interaction.

ACKNOWLEDGMENT

We are grateful to the Indo-French Center for the Promotion of Advanced Research (India)/Centre Franco-Indien pour la Promotion de La Recherche Avancée (France) for the financial assistance for the project.

*bspujari@physics.unipune.ernet.in

[1] M. Reed, Sci. Am. (Int. Ed.) **268** (1), 118 (1993).
[2] R. C. Ashoori, Nature (London) **379**, 413 (1996).
[3] S. M. Reimann and M. Manninen, Rev. Mod. Phys. **74**, 1283 (2000).
[4] A. I. Ekimov, A. L. Efros, and A. A. Onushchenko, Solid State Commun. **56**, 921 (1985).
[5] G. W. Bryant, Phys. Rev. Lett. **59**, 1140 (1987).
[6] S. A. Akbar and I. H. Lee, Phys. Rev. B **63**, 165301 (2001).
[7] E. Räsänen, H. Saarikoski, V. N. Stavrou, A. Harju, M. J. Puska,

and R. M. Nieminen, Phys. Rev. B **67**, 235307 (2003).
[8] K. Hirose and N. S. Wingreen, Phys. Rev. B **59**, 4604 (1999).
[9] S. Tarucha, D. G. Austing, T. Honda, R. J. van der Hage, and L. P. Kouwenhoven, Phys. Rev. Lett. **77**, 3613 (1996).
[10] S. M. Reimann, M. Koskinen, and M. Manninen, Phys. Rev. B **59**, 1613 (1999).
[11] M. Kalinski, L. Hansen, and D. Farrelly, Phys. Rev. Lett. **95**, 103001 (2005).
[12] E. Lee, A. Puzder, M. Y. Chou, T. Uzer, and D. Farrelly, Phys. Rev. B **57**, 12281 (1998).
[13] C. Yannouleas and U. Landman, Phys. Rev. Lett. **82**, 5325 (1999).
[14] A. Harju, S. Siljamäki, and R. M. Nieminen, Phys. Rev. B **65**, 075309 (2002).
[15] W. M. C. Foulkes, L. Mitas, R. J. Needs, and G. Rajagopal, Rev. Mod. Phys. **73**, 33 (2001).
[16] A. Ghosal, A. D. Güçlü, C. J. Umrigar, D. Ullmo, and H. U. Baranger, Nat. Phys. **2** (5), 336 (2006).
[17] A. Ghosal, A. D. Güçlü, C. J. Umrigar, D. Ullmo, and H. U. Baranger, arXiv:cond-mat/0702666v1 (unpublished).
[18] D. G. Austing, S. Sasaki, S. Tarucha, S. M. Reimann, M. Koskinen, and M. Manninen, Phys. Rev. B **60**, 11514 (1999).
[19] C. Creffield, W. Häusler, J. Jefferson, and S. Sarkar, Phys. Rev. B **59**, 10719 (1999).
[20] M. Şahin and M. Tomak, Phys. Rev. B **72**, 125323 (2005).
[21] J. L. Movilla and J. Planelles, Phys. Rev. B **71**, 075319 (2005).
[22] E. Räsänen, J. Kösnemann, R. J. Haung, M. J. Puska, and R. M. Nieminen, Phys. Rev. B **70**, 115308 (2000).
[23] B. Reusch and R. Egger, Europhys. Lett. **64**, 84 (2003).
[24] P. Hohenberg and W. Kohn, Phys. Rev. **140**, A1133 (1965).
[25] W. Kohn and L. J. Sham, Phys. Rev. **136**, B864 (1964).
[26] B. Tanatar and D. M. Ceperley, Phys. Rev. B **39**, 5005 (1989).
[27] G. Finkelstein, P. I. Glicofridis, R. C. Ashoori, and M. Shayegan, Science **289**, 90 (2000).
[28] E. P. Wigner, Phys. Rev. **46**, 1002 (1934).
[29] A. V. Filinov, M. Bonitz, and Y. E. Lozovik, Phys. Rev. Lett. **86**, 3851 (2001).
[30] B. Reusch, W. Häusler, and H. Grabert, Phys. Rev. B **63**, 113313 (2001).
[31] R. Egger, W. Häusler, C. H. Mak, and H. Grabert, Phys. Rev. Lett. **82**, 3320 (1999).
[32] S. M. Reimann, M. Koskinen, and M. Manninen, Phys. Rev. B **62**, 8108 (2000).
[33] M. Evaldsson and I. V. Zozoulenko, Phys. Rev. B **73**, 035319 (2006).
[34] W. G. van der Wiel, S. De Franceschi, J. M. Elzerman, S. Tarucha, L. P. Kouwenhoven, J. Motohisa, F. Nakajima, and T. Fukui, Phys. Rev. Lett. **88**, 126803 (2002).
[35] It has been noted in Ref. 7 that these oscillations can be picked up by SDFT and not by DFT.